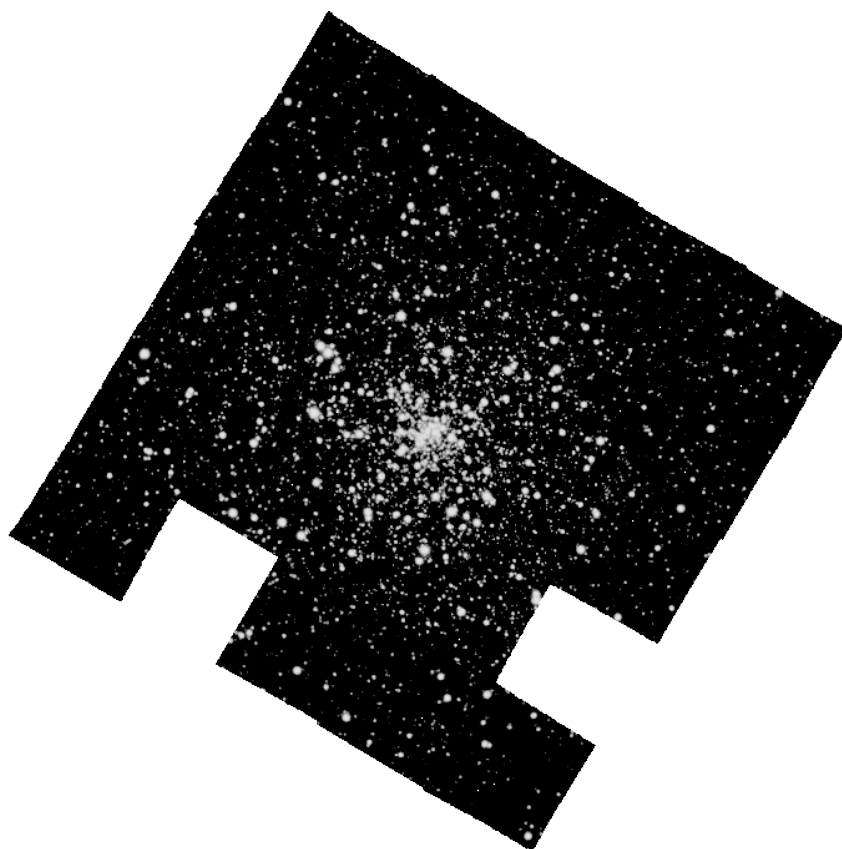


Master ASEP
Manuel Pichardo Marcano

MUSE integral field unit observations of the compact objects in the globular cluster
NGC 6397



Advisor : Dr. Natalie Webb, IRAP.

Abstract

Globular clusters are very old groups of stars. Due to their age and the gravitational interactions dominating the dynamics of the clusters, they are home to a significant fraction of compact binaries. The formation and evolution of these kinds of binaries is still not completely understood. Of special interest is the globular cluster NGC 6397 as it is the closest core collapsed cluster and has therefore been extensively studied with instruments like Chandra, Hubble Space Telescope, and more recently in the optical with the Multi Unit Spectroscopic Explorer (MUSE), installed on the Very Large Telescope (VLT). Integral field spectrographs, like MUSE, have many advantages compared to traditional long slit spectroscopy, as spectra are obtained for every pixel and thus every object in the large field of view ($1' \times 1'$). Here we present analysis of the compact binary population in NGC 6397 taken with MUSE. The goal is to further understand the characteristics of the proposed bimodal population of cataclysmic variables in the cluster, which have been suggested to be of primordial and dynamically formed origin. In this work we were able to spectroscopically confirm two new CV candidates as well as retrieve the spectra of three previously identified CVs. Spectral analysis on the extracted spectra allow us to estimate the mass ratio for a sample of the identified CVs. We also were able to compare the magnitude in the R band with previous observation of NGC 6397 to determine if any of the CVs were observed during an outburst. From the spectral emission and absorption lines were were also able to estimate the possible type of the companion and examine the magnetic nature of the CVs. We specifically searched for Helium II lines as signature of magnetism, and Titanium Oxide lines from a M type companion. We show that this shallow observation of NGC 6397 with MUSE is a good starting point to finally obtain optical spectral of compact objects in globular clusters but that with deeper observations a more complete study of the CVs and other compact objects can be carried out.

Contents

1	Introduction	4
1.1	Location, Location, Location	4
1.2	Compact Objects or Stellar remnants	4
1.2.1	White Dwarfs	5
1.2.2	Neutron Stars	5
1.2.3	Black Holes	5
1.3	Compact Binaries	6
1.3.1	The Gravitational Potential	6
1.3.2	Binary Evolution	8
1.3.3	Accretion	9
1.3.4	Cataclysmic Variables (CVs)	9
1.3.4.1	Classical Novae (CN)	10
1.3.4.2	Dwarf Novae (DN)	10
1.3.4.3	Novae-like (NL)	11
1.3.4.4	Polars	11
1.3.4.5	Intermediate Polars (IPs)	11
1.3.5	X-Ray binaries	11
1.3.5.1	Low-mass X-Ray Binaries	11
1.3.5.2	High-mass X-Ray Binaries	12
1.4	Globular Clusters	12
1.4.1	CVs in Globular clusters	12
1.4.2	NGC 6397	13
2	Observation and data reduction	15
2.1	VLT/MUSE	15
2.2	Processed and Raw data	15
2.2.1	Data Reduction	16
2.2.2	Spectral extraction and analysis	18
3	Results	19
3.1	Cataclysmic Variables	19
3.1.1	Variability	19
3.1.2	Mass ratio	19
3.1.3	Radial Velocity	20
3.2	Low-mass X-ray Binary	21
4	Discussion and Conclusions	24
4.1	Primordial CVs	24
4.2	Periods	24
4.3	Magnetism and dwarf novae	25

5	Future Work	26
5.1	Follow up Observation	26
5.2	Data analysis	26
5.2.1	Optimal Spectra Extraction	26
5.2.2	Short Term variability	26
5.2.3	Processed data	26
5.3	Reproducibility	27
5.3.1	Continuous Analysis	27
5.3.2	Cloud Computing	27

Chapter 1: Introduction

1.1 Location, Location, Location

Important in real estate, but also seemingly an important factor to take into account when studying compact objects in binary systems. It seems that, like with people, where you were born plays a role in your evolution. This seems to be true for cataclysmic variables (CVs), the kind of compact binary system that we will explore in more detail in the present work. Our goal is to try to understand the formation of these kinds of systems when they are formed in a crowded and high density environment (like in a cluster of stars), and when you give them enough time to evolve and interact with other stars (like in a globular cluster).

Now that we have defined our broad goal let's take a step back and explore in more detail what are compact objects, their different types, and the different ways they can interact with each other and other types of stars (Sec. 1.2). That section will lead us to the discussion of where and how we expect to find them, and what can we learn by studying them in the different environment where they form (sections 1.4).

1.2 Compact Objects or Stellar remnants

Compact objects, as their name suggest, are very massive and dense objects formed from the remains of a dying stars; hence their other name, 'stellar remnants'. They come in three main flavors, each following a different formation mechanism that is mainly determined by the mass of the progenitor star (de Boer & Seggewiss, 2008). The different types are neutron stars (NS), black holes (BH), and white dwarfs (WD) (see sections 1.2.1, 1.2.2 and 1.2.3). Besides these three, other possible exotic types of stars have been proposed; including quark stars, boson stars, and Thorne-Zytkow objects. These will not be discussed in this work as there is still a lack of observational evidence concerning their existence. The reader is referred to Madsen (1999) to discover more about these particular kind of proposed stars.

Of the three confirmed compact objects (neutron stars, white dwarfs and black holes), we will focus on the first two (NS and WD). They belong to a class of objects called "degenerate objects". These are objects for which the supporting force comes from the degeneracy pressure of fermions¹. In the case of a white dwarf the pressure is provided by the degenerate electron gas (Fowler, 1926), and for a neutron stars, clearly, the neutrons cause the repulsive pressure (Oppenheimer & Volkoff, 1939).

The next subsection will list some of the characteristics of NS, and WD (both when they are found in isolation (sec 1.2.1 and 1.2.2) or in a binary system, Sec. 1.3). Black holes will be briefly discussed for the sake of completeness.

¹Fermions are particles with half-integer spin. They follow the Fermi-Dirac statistics, thus obey the Pauli exclusion principle. The consequence of the exclusion principle is that two fermions cannot occupy the same quantum state. This is the origin of the degeneracy pressure.

1.2.1 White Dwarfs

White dwarfs are the most common end product in the evolution of stars. Around 90% of stars will evolve to become WDs (Koester & Weidemann, 1980). This includes all main sequence stars ² (MS) with a mass between ~ 0.6 and $\sim 8 M_{\odot}$ (Koester & Chanmugam, 1990). The resulting white dwarf will have a mass between ~ 0.3 and $\sim 1.4 M_{\odot}$ (Prada Moroni & Straniero, 2009; Chandrasekhar, 1931), the average mass being $\sim 0.7 M_{\odot}$ (Koester & Chanmugam, 1990). All this mass is contained in a radius of about $\sim 0.01 R_{\odot}$ (Kepler & Bradley, 1995). These are average values, but the mass-radius relation for a white dwarf is plotted in Fig 1.2. If we take the mean values mentioned before this gives a mean density of 10^9 kg/m^3 . This mass-radius relation will be composition dependent and it depends, for example, on the element dominating the atmosphere composition (Hamada & Salpeter, 1961). About 80% of all white dwarfs have hydrogen-dominated atmospheres (spectral type DA), but there exists a second class where helium dominates the atmosphere composition (spectral types D0, DB, DC, DZ and DQ)(Wickramasinghe & Ferrario, 2000; Koester & Chanmugam, 1990). White dwarfs are also known to be magnetic. Surface magnetism ranges from about 10^5 to 10^9 G (Suh & Mathews, 2000). Isolated magnetic white dwarfs represent $\sim 5\%$ of all WDs. See Wickramasinghe & Ferrario (2000) for a review on magnetism in WDs and for more details on the physics of white dwarfs the reader is referred to Koester & Chanmugam (1990) and Kepler & Bradley (1995).

1.2.2 Neutron Stars

Neutron stars are produced from the gravitational collapse of a massive star ($> 8 M_{\odot}$)(de Boer & Seggewiss, 2008) at the end of its life. The type II supernova produced by this collapse, leaves behind a dense and massive core (~ 12 kilometers in radius (de Boer & Seggewiss, 2008)), but up to $\sim 2 M_{\odot}$ (this limit being model dependent, see Lattimer & Prakash (2007)). For comparison with white dwarfs a sample mass-radius relation for a NS (red) is plotted along with that of a white dwarf (blue) in Fig 1.2. Like WDs, neutron stars are also known to be magnetic. The range in their magnetic field being from $\sim 10^7 - 10^{13}$ G. There also exist some neutron stars with unusually strong magnetic fields ($B \sim 10^{14} - 10^{15}$ G) and are called "magnetars" (Duncan & Thompson, 1992). For a review on magnetic fields in neutron stars see Reisenegger (2005).

Neutron stars are mainly composed of neutrons and a thin atmosphere of a few cm of hydrogen or helium (Zavlin et al., 1996). We have come a long way since the first proposition of their existence, but there is still a lot of uncertainty concerning their interiors and a lot of existing conflicting models (Lattimer & Prakash, 2007). Since we have had observational evidence on their existence (Hewish et al., 1968) efforts have been made to constrain the different models. Figure 1.1 shows a visual summary of some of the different models proposed. There are many ways that we can observationally constrain these models, spectroscopy being one of them.

1.2.3 Black Holes

Black holes are the fate of collapsing matter when no force, including the degeneracy pressure of neutrons, is enough to repel gravitational attraction. Black holes, like neutron stars and white dwarfs, can be the result of the collapse of a single main sequence star. Stars with an initial mass $\gtrsim 20 M_{\odot}$ can end their lives as a black hole (Heger et al., 2003), but the initial mass is not the only factor that comes into play. For example, the formation of the black hole will depend also on the metallicity of

²Main sequence stars are those that are burning hydrogen in their cores.

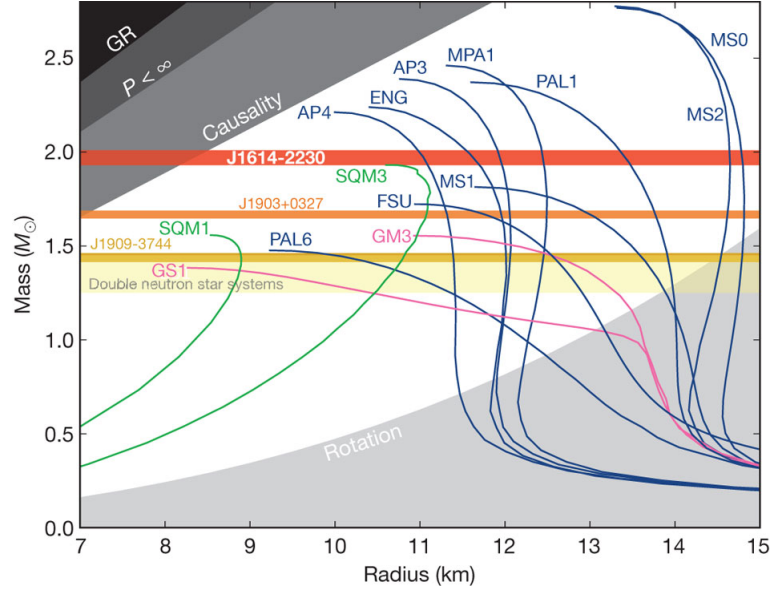


Figure 1.1: The plot shows non-rotating mass versus physical radius for several typical equation of states. Blue, nucleons; pink, nucleons plus exotic matter; green, strange quark matter from (doi:10.1038/nature09466)

the star and/or binarity. See Heger et al. (2003) and (Brown et al., 2000) for details on the evolution of high mass stars and the different formation path leading to a black hole from a single collapse star.

To compare the physical characteristics of a black hole with other compact objects we can define the gravitational radius or Schwarzschild radius of a black hole. This is the radius to which a given spherical and non-rotating mass needs to be reduced to get a escape velocity equal to the speed of light. This translates to:

$$r = \frac{2MG}{c^2} \quad (1.1)$$

An estimate of the lowest mass of a black hole is the maximum possible mass for a neutron star, this is $\sim 3M_{\odot}$ (Rhoades & Ruffini, 1974). With the formula above we can get a rough estimate on the size of a stellar mass black hole. A mass of $3 M_{\odot}$ and the formula above gives an equivalent Schwarzschild radius of about 9 km.

1.3 Compact Binaries

Compact binaries are those binaries where at least one of their components is a compact object (WD, NS or BH). In this section we will start by discussing some of the basic concepts of binary evolution, follow by a discussion on mass exchange between binary components, and finish by looking in more detail at some specific examples of compact binaries that are relevant to this study.

1.3.1 The Gravitational Potential

The total potential of a binary system is the sum of the gravitational and the rotational potential. To get an analytical solution we can assume a model in which the resulting disturbing potential is due to

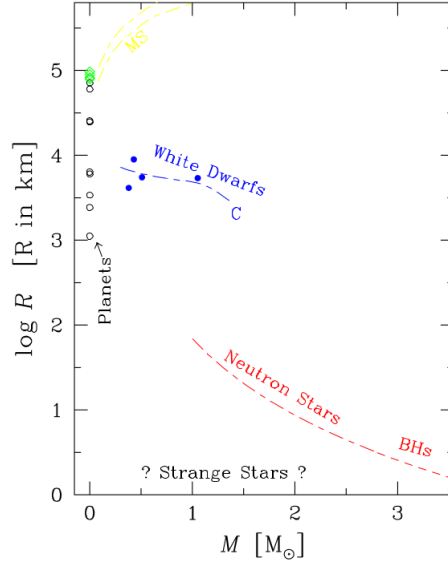


Figure 1.2: Mass-radius relation for different objects (de Boer & Seggewiss, 2008).

the presence of two point masses, M_1 (or the primary) and M_2 (also called the secondary). Moreover, we assume a co-rotating Cartesian reference frame (x, y, z) with origin at the primary M_1 ; whose x-axis is in the direction joining the two point masses; and the z-axis is perpendicular to the orbital plane. The total potential, Ψ at an arbitrary point $P(x, y, z)$ then reads:

$$\Psi = -G \frac{M_1}{\sqrt{x^2 + y^2 + z^2}} - G \frac{M_2}{\sqrt{(R-x)^2 + y^2 + z^2}} - \frac{\omega^2}{2} [(x - \mu R)^2 + y^2] \quad (1.2)$$

where G is the gravitational constant, R represents the separation between the point masses, and $\mu = M_2/(M_1 + M_2)$. We further assume that the binary orbit is Keplerian, thus the orbital frequency is given by:

$$\omega^2 = G \frac{M_1 + M_2}{R^3} \quad (1.3)$$

Taking into account the assumptions the surfaces generated by eq 1.2 are called *Roche Equipotential*³. Fig 1.4 show such equipotential surfaces (x, y plane). Of special interest are two regions on the graph:

- The inner Lagrangian point L_1 . This is where all the forces cancel out.
- Critical or **Roche lobe**. The surface that have the potential equal to the L_1 potential.

The Roche lobe has the property that inside the lobe of an object, any material will be gravitationally bound to that object. With this knowledge we can classify binary systems into three groups:

1. **Detached systems**. If the volumes of both components are significantly smaller than their Roche lobe.

³We are neglecting here the radiation pressure from the stars. For more details on Roche Potentials Including Radiation Effects see Schuerman (1972)

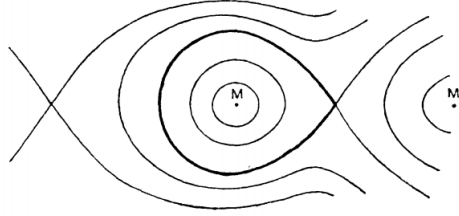


Figure 1.3: Geometry of the Roche surfaces. The Roche lobe is marked in bold lines (Kopal, 1959).

2. **Semi-detached systems.** Where one of the components fills its Roche lobe.

3. **Contact systems.** Where both components appear to fill their respective Roche lobes.

This classification scheme was first suggested by (Kopal, 1955) and developed in detail in a comprehensive monograph in 1959 (Kopal, 1959).

1.3.2 Binary Evolution

In this work we are mostly interested in the formation of semi-detached compact binary systems. In this section we briefly explore a possible scenario for its formation.

These kinds of systems can be formed from two previously detached MS stars binaries that evolve on different timescales due to their different masses. This can be seen noticing that the luminosity, L , indicates the rate of consumption of nuclear fuel; and the nuclear fuel repository is proportional to the mass, M . This gives us a rough estimates of the nuclear timescale of a star given by:

$$\tau \propto \frac{M 6 \times 10^{18} \text{ergs g}^{-1}}{L} \quad (1.4)$$

Where L is the luminosity, M is the mass, and $6 \times 10^{18} \text{ergs g}^{-1}$ is the energy release fusing a gram of hydrogen to helium. Moreover, with the mass-luminosity relation $L/L_{\odot} = (M/M_{\odot})^{\alpha}$, where $\alpha \gtrsim 3$ (e.g. de Boer & Seggewiss, 2008), we can conclude that in a system starting with two detached main sequence stars, the more massive one will leave the main sequence faster. As it expands after it leaves the main sequence in the process of becoming a compact object, a common envelope around both stars will be formed. This allows the two stars to get close enough to interact. The envelope is then expelled, leaving behind a binary system with a compact object and an evolved main sequence star. The old main sequence star in the binary as it continues to evolve will expand and fill its Roche lobe, allowing for accretion into the compact object to happen. The process is more complex and, among other things, depends on the initial mass of both stars and initial binary separation. For example, a binary system starting with a $2 M_{\odot}$ and a $1 M_{\odot}$ star can produce a white dwarf accreting from a late-type main sequence star (Kippenhahn et al., 1967; De Loore & Doom, 1992). A system starting with a $15 M_{\odot}$ and $2 M_{\odot}$ will become a neutron star accreting from a low mass main sequence star (van den Heuvel, 1976). In the case of starting masses of $20 M_{\odot} + 8 M_{\odot}$ this can produce a neutron star (or black hole) accreting from a high mass main sequence star (van den Heuvel, 1976). The details on the evolution of close binaries can be found in Postnov & Yungelson (2014). and (de Boer & Seggewiss, 2008)

In the next section we will see in some detail how the accretion can take place once the compact binary is formed due to stellar evolution of their constituents.

1.3.3 Accretion

In the Roche overflow scenario we have incoming gas from the secondary star. After it passes through the L_1 point we assume a ballistic behavior completely governed by the gravitational potential of the compact object. This is justified by the fact showed by Lubow & Shu (1975) that the stream is supersonic and we can ignore pressure. We can also assume that the incoming speed must be small. This is safe to assume if the accretion is due solely to overflow and thus the velocity is of the order of the sound speed in the atmosphere of the secondary star. This speed is much slower than the orbital speed of the binaries, and lower than the velocities acquired during the fall. This simplification means that we can treat the Roche lobe as a zero velocity surface. Meaning that the motion of the gas can be approximated as the trajectory of a test particle released from rest with an initial angular momentum from L_1 . This creates an elliptical orbit of the stream around the primary star (Fig 1.4 a). As the gas flow continues it will impact itself. This causes the flow to modify its orbit to that of the lowest energy at a specific angular momentum (we assume angular momentum is conserved). Of course the orbit of lowest energy at a given angular momentum is a circular one (see Fig 1.4 b). This creates a ring around the compact object. We can estimate the radius of this ring by again invoking the assumption that no angular momentum is lost in the process. The angular momentum at L_1 would be given by $R_{L1} V_{orbit}$ (where R_{L1} is the distance from the secondary to L_1). Knowing that $\omega = (2\pi)/\text{Period}$ and equating the angular momentum at L_1 to the angular momentum of a Keplerian orbit at R_{ring} we get:

$$\frac{R_{ring}}{R} = \left(\frac{R_{L1}}{R} \right)^{\frac{1}{4}} (1 + q) \quad (1.5)$$

where I used eq 1.3 to simplify the answer by canceling some constants. This is called the *circularization radius*. After a ring is formed (Fig 1.4 b), as first indicated in Lynden-Bell & Pringle (1974), any viscous processes will cause the ring to spread to conserve angular momentum (Fig 1.4 d) The nature of these viscous torques won't be discussed here. For a review on the topic see Frank et al. (2002) and Verbunt (1982). Roche lobe overflow is not the only type of accretion, others include wind accretion or Bondi accretion. In this work, unless otherwise stated, accretion will mean accretion by Roche lobe overflow. See the references cited above for more details on other type of accretion.

Now that we studied briefly accretion and see how it can happen in semi-attached binaries, in the next section we will discuss two specific examples of this happening. One where the accretion is onto a white dwarf (Cataclysmic Variable), and the other where the accretion is onto a neutron star or a black hole (X-Ray binaries).

1.3.4 Cataclysmic Variables (CVs)

Cataclysmic variables are semi-detached binary systems comprised of a white dwarf (primary star) and typically a low mass main sequence star. CVs are generally classified into two groups. Magnetic CVs ($\sim 10^6 - 10^8$ G) and nonmagnetic CVs ($B < 0.01$ MG). Magnetic CVs constitute about 25% of the known CV population (Balman, 2012). CVs have typical period in the range of 1-10 hrs. In this period range the distribution is not uniform. In fact, there is a well defined region ($2.3 \lesssim P_{orb}(h) \lesssim 2.8$) where there is a deficiency of non-magnetic CVs. This is called the 'period gap'. CVs above the period gap are assumed to lose angular momentum via magnetic braking, and CVs below the period gap lose angular momentum purely by gravitational radiation. The magnetic braking stops when the secondary becomes fully convective. At this point the accretion stops and the system becomes a detached one.

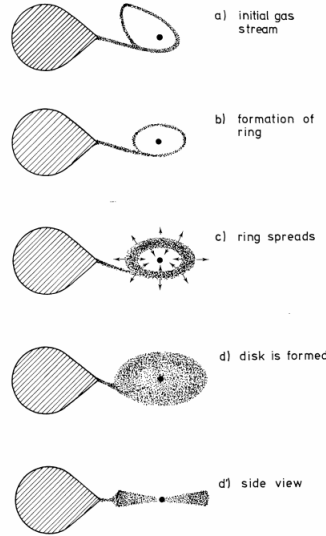


Figure 1.4: Schematic illustration of the formation of an accretion disk around a compact binary (Verbunt, 1982).

Angular momentum is then lost solely via gravitational radiation. This shrinks the orbit and brings the two stars into contact resuming the mass transfer (e.g. Warner, 2003).

CVs can be observed in many wavelengths. This includes radio observation of jets (Körding et al., 2008); (Coppejans et al., 2015)), optical and UV observation of the accretion disks (Kinney, 1994), and X-rays ($\sim 0.5 - 2.5$ keV) from the infalling plasma onto the white dwarfs (Verbunt et al., 1997). As their name suggests these are very variable systems, specially the nonmagnetic CVs). These variabilities are due either to instabilities in the accretion disk, referred to as dwarf novae (Osaki, 1974), or unstable burning of hydrogen at their surface, called nova (Starrfield et al., 2016). We will discuss the outburst caused by these instabilities, and the nature of the magnetic CVs by presenting the classification of CVs and exploring the taxonomy of these objects.

1.3.4.1 Classical Novae (CN)

When the surface of an accreting white dwarf becomes hot enough ($\sim 10^8$ K, e.g. Starrfield et al. (2016)), nuclear fusion can take place and a thermonuclear runaway happens. This creates a violent explosion capable of ejecting material (mean mass of $\sim 2 \times 10^{-4} M_{\odot}$) at high velocities ($\sim 10^2 - 10^3$ km s $^{-1}$) (Gehrz et al., 1998; Shara, 1989). These outburst are fairly easy to detect since they cause a substantial increase in brightness (typically ~ 12 magnitudes in optical, Shara 1989). A CV observed erupting in such a way is classified as a *classical nova (CN)*. Classical novae are seen to erupt only once. If a previously recognized CN erupts again as a CN they are called recurrent novae.

1.3.4.2 Dwarf Novae (DN)

A dwarf nova outburst is caused by instabilities in the accretion disk. This is predicted to happened in non-magnetic CVs with low accretion rates (Osaki, 1974). CVs that show these outbursts are classified as dwarf novae. The outburst from a dwarf nova is not as violent as the one from a classical novae. The magnitude change is only of about 2-5, and no material is ejected. They also, unlike classical novae,

are periodic in nature on times scales of weeks to years depending mainly on the accretion rate (Shara, 1989). Probably the best known example of a dwarf nova is the variable star SS Cygni (Cannizzo & Mattei, 1998).

1.3.4.3 Novae-like (NL)

Another classification of white dwarfs is the novae-like. They are CVs that seem to have stable accretion, thus not undergoing dwarf novae outburst and having a bright stable disk. They represent the 'non-eruptive' CVs.

1.3.4.4 Polars

Polars are CVs with a strong magnetic field. The value of the magnetic field is usually between 20 MG to 230 MG (Balman, 2012). The field in polars is so strong that it couples to the field of the donor and forces the WD to corotate with the companion. The presence of the strong magnetic field also disrupt the accretion disk. In the case of Polars the accretion flow is redirected so it takes place at the magnetic pole guided by the magnetic field lines. This causes X-ray radiation (produced by shocks and bremsstrahlung) and strongly circular polarized ($> 10\%$) cyclotron radiation in the optical and infrared bands (Cropper, 1990). This polarized emission is the reason for the name Polars (Krzeminski & Serkowski, 1977). The polarization was the first clue on the magnetic nature of these type of systems. It was first discovered for AM Herculis (AM Her), now the prototype polar CV (Tapia (1977)). Polar systems are often referred to as AM Her-like system. This kind of systems represent 63% of the magnetic CV population (Balman, 2012).

1.3.4.5 Intermediate Polars (IPs)

Intermediate polars are the second kind of magnetic CVs. In this type the magnetic field is weaker ($\sim 1 - 20\text{MG}$). The weaker strength of the magnetic fields means that the accretion disk is not entirely dominated by the magnetic field, and the system is asynchronous, so the WD does not corotate with the binary. This kind of systems represent 37% of the known magnetic CV population (Balman, 2012). An extensively studied member of this class is DQ Her. DQ Her is sometimes refer as a subclass of IPs (IPs with period $\lesssim 120$ s), or even as a synonym for IPs (Patterson, 1994; Warner, 2003).

1.3.5 X-Ray binaries

X-Ray binaries are a subclass of compact binaries where the accretor is either a neutron star or a black hole. They can be classified into two regimes depending on the type of the donor star. If the donor or secondary is a late-type star it is called a low-mass X-ray binary; if it is an early-type star they are called high-mass X-ray binaries.

1.3.5.1 Low-mass X-Ray Binaries

Low-mass X-ray binaries (LXMBs) are Roche-lobe overflow binary stars consisting of a neutron star or a black holes accreting from a low-mass ($\lesssim 1.5M_{\odot}$) donor. The donor can be a main sequence star or even a white dwarf (Tauris & van den Heuvel, 2006).

In the case of a LMXB, since the accretor (NS or BH) has a higher mass than the white dwarf in a CV, the energy release in the accretion process is higher. This means that we get more powerful X-ray

radiation from LMXB (up to ~ 10 keV) (Tauris & van den Heuvel, 2006). The period can range from 11 minutes to 17 days, and like CVs they can show magnetism ($\sim 10^9 \sim 10^{11}$ G) (Tauris & van den Heuvel, 2006).

1.3.5.2 High-mass X-Ray Binaries

High-mass X-ray binaries (HMXB) are the second class of X-ray binaries. In the case of an HMXB the donor star is a young early-type main sequence star. This usually means a O or B spectral type with a mass $> 10M_{\odot}$ (e.g. Tauris & van den Heuvel, 2006). Contrary to the LMXB the accretion is not entirely due to Roche overflow, it can be due to the high velocity winds produced by the donor star. And also unlike the LMXB this systems tend to show stronger magnetic fields and stronger X-ray radiation (ibid.)

1.4 Globular Clusters

Globular clusters (GCs) are very old and dense gravitationally bound groups of stars. Their age is generally around 10 Gyr (Meylan & Heggie, 1997) and typically contain $\sim 10^6$ stars (Knigge, 2012). Due to their age we expect to find compact objects, and the high density environment is ideal for the formation of compact binaries. In fact the formation of these binaries plays an important role in the evolution of globular clusters. Globular clusters are known to have a phase where their evolution is governed by the formation and dynamics of binaries in their cores. This is called the "binary burning" phase. In this phase the gravitational collapse in a GC can be balanced by energy produced via dynamical hardening of binaries (binaries become more strongly bound) in the core (e.g. Hut et al., 1992). The importance of this effect is far from being completely understood, and a better understanding on the compact binaries in GC is needed. The search for these compact binaries have been fructiferous leading to the detection of X-ray binaries and Cataclysmic Variables in several globular clusters (e.g. Maccarone & Knigge, 2007). But still the formation and evolution of these kinds of binaries is still not completely understood, and many uncertainties remain. Of special interest for this project are the cataclysmic variables in globular clusters. In the next subsection we will make a brief overview on the current knowledge on the subject and state the current open questions that we mean to address in this project.

1.4.1 CVs in Globular clusters

Cataclysmic Variables are tracers of the dynamical evolution in globular clusters. Their number and spatial distribution can give us a clue on the past of the globular cluster, and help us constrain models of stellar and dynamical evolution. CVs are expected to be the most abundant compact binary based on the fact that the white dwarf is the most common fate of stars. Theoretical modeling predicts ~ 100 CVs in a given GC (varying a bit with the cluster metallicity and stellar density, see Ivanova et al. (2006)). They are expected to form two distinctive groups based on their formation mechanism, primordial CVs and dynamically formed CVs (e.g. Hut et al., 1992). Primordial are those CVs that formed from primordial binaries that didn't get destroyed through a physical collision in the cluster. The dynamically formed CVs are those formed via dynamical encounters with other members in the cluster. This includes tidal capture, exchange interactions and collision events. For example a dynamically formed CV can form through the tidal capture of a MS star by a WD, or by a system resulting from the collisions between a red giant and a MS star (Ivanova et al., 2006).

The problem with the theoretical picture described above is that hitherto there is no observational evidence of two distinct CV population in globular clusters. The lack of detection of these two predicted populations raises the question **Where are all the primordial CVs?**. The number can be theoretically predicted ($\sim 37\%$ of all CVs in a GC (Ivanova et al., 2006)), but we need observational evidence to constrain the theoretical models. The dense environment in which they form and the possibility that CVs are formed through dynamical interaction can result in a differentiation of the binary population from the galactic field population. For example, the result of these dynamical processes is that in the dense cores of GCs, binaries are strongly depleted and their period distribution is expected to be different from that of a field population as in the field almost all are primordial and not dynamically formed CVs (Ivanova et al., 2005). So the questions becomes, **What is the period distribution of CVs in Globular Clusters?**. In the Galactic field the period distribution has been well studied. The period of CVs in the field is governed by magnetic braking ($P_{orb} \gtrsim 3h$), and gravitational radiation ($P_{orb} \lesssim 2h$) (Robinson, 1983). The period distribution in GC is still not well understood mainly due to lack of observational data. There are only 15 CVs with known periods from a small sample of 5 globular clusters (Knigge, 2012). Another difference between fields and GC CVs that has been proposed is that CVs in GCs tend to be primarily magnetic in nature (Grindlay, 1999). This will explain the lack of observed dwarf novae outburst in CVs (Shara et al., 1996) and the high X-ray luminosity of GC CVs, compared to fields CVs (Verbunt et al., 1997). However data is scarce to support that argument and the questions remain: **Are globular clusters in CVs mainly magnetic in nature and where are all the dwarf novae?**

With the questions mentioned above in mind, in this project we studied the population of Cataclysmic Variables in a nearby globular cluster, NGC 6397. The next section describes the most important characteristic of NGC 6397 and the previous studies done regarding its compact binary population.

1.4.2 NGC 6397

NGC 6397 is the closest (2.4 kpc) core collapse⁴ globular cluster (Harris, 1996; McLaughlin & van der Marel, 2005) with center at RA(J2000): $17^h 40^m 42.09^s$ and Dec(J2000): $-53^\circ 40' 27.6''$ (Harris, 1996). A globular cluster can be characterize by three main radii. These are the core radius (r_c), half-mass (or half-light) radius (r_h), and the tidal radius (r_t). The core radius is the distance at which the apparent surface luminosity has dropped by half, the half-mass radius is the radius of the sphere containing the innermost half of the mass, and finally the tidal radius is the distance at which the gravitational influence of the clusters extents. For NGC 6397 these values are: $r_c = 0.05'$, $r_h = 2.90'$ and $r_t = 15.81'$ (Harris, 1996).

Due to its proximity NGC 6397 has been extensively studied in different wavelengths. The observation by Cool et al. (1993) with the ROSAT instrument was the first one to detect X-rays sources in NGC 6397. This was followed by a photometric study with the Hubble Space Telescope wide field and planetary camera (WFPC) confirming the first three CVs candidates in NGC 6397 (Cool et al., 1995). Since then follow up observations with Chandra (Grindlay et al., 2001; Bogdanov et al., 2010) and with Hubble (Taylor et al., 2001; Grindlay, 2006), both with the faint object spectrograph and with the advanced camera for surveys (ACS), have found a total of 15 CVs candidates (Cohn et al., 2010). From these currently known candidates only 4 have been spectroscopically confirmed (Grindlay et al.,

⁴Core collapse are clusters showing a power-law slope in their surface brightness profile near the center due to the gravothermal instability (Antonov, 1962; Lynden-Bell & Wood, 1968; Lynden-Bell & Eggleton, 1980). In contrast to other isothermal sphere models showing a more flatten brightness profile in the center (e.g. King (1966))

1995; Edmonds et al., 1999), and the period is known for only two of them (Kaluzny & Thompson, 2003; Kaluzny et al., 2006).

In this work our goal is to exploit new data available from NGC 6397 and increase our understanding of CVs in globular clusters. We particularly try to extend the sample size of spectroscopically confirmed CVs and study their properties (e.g. period, mass and variability). In the next chapter we will discuss the nature of the observations and data used for the analysis.

Chapter 2: Observation and data reduction

2.1 VLT/MUSE

NGC 6397 was observed with the Multi Unit Spectroscopic Explorer (MUSE) at the Very Large Telescope (VLT) of the European Southern Observatory (ESO) at Paranal, Chile. MUSE is an integral field Unit (IFU). MUSE works by separating the full field of view ($1' \times 1'$) into 24 sub-fields ($2.5'' \times 60''$). Each of these 24 is then processed by 24 identical but independent integral field units (IFU). Each IFU consists of an image slicer, a spectrograph and a CCD. Each IFU illuminates a $4k \times 4k$ CCD after slicing the light into 48 slit-like slices (with size $\sim 15'' \times 0''.2$), and decomposing it via a volume phase holographic grating (Barden et al., 1998). The grating achieves a spectral resolution of 1750 at 4650 Å to 3750 at 9300 Å. The data from the 1152 slices is then reconstructed into a $1' \times 1'$ datacube (two spatial and one wavelength axis) with a $0''.2$ spatial resolution covering from 4750 Å to 9350 Å sampled at 1.25 Å (Bacon et al., 2010).

NGC 6397 was observed during the third commissioning period (ESO Programme ID 60.A-9100(C) Bacon et al. (2014)). The observations were taking from July 26th to August 3rd, 2014. The observations covered the central part of NGC 6397 ($\sim 3''.5$ from the cluster center see Fig 2.1). The dataset consists of 23 different pointings of MUSE with short exposure times ranging from 25-60 seconds. In total they obtained 127 exposures of the 23 different $1' \times 1'$ regions (see Fig 2.1). This gives a total integration time of 95 minutes for all the observed part of the cluster.

2.2 Processed and Raw data

The primary goal of the MUSE observation of NGC 6397 was to create the first comprehensive Hertzsprung-Russell diagram with a sample of over 12 000 spectra (Husser et al., 2016). The large number of spectra obtained allowed them to study the kinematics of the globular cluster with the goal to probe the presence of a central black hole in the cluster (Kamann et al., 2016). This data is publicly available through the *MUSE Science Web Service*¹. The website contains advanced science products such as reduced datacubes, source catalogs and software tools. For NGC 6397 the spectra of the globular cluster NGC 6397 as published in the studies mentioned above (Husser et al. (2016) and Kamann et al. (2016)) are provided. They provide all the obtained spectra with a signal-to-noise ratio of five or larger, i.e. 14271 spectra in total. For our goal to study the CVs in the globular clusters the data wasn't enough as it mainly covers the range from main sequence to the tip of the red giant branch². Our approach in this project was to work with the raw science data. The science data can be obtained from the ESO Science Archive Facility. As stated in the ESO Data Access Policy³ all science data is made publicly available through the science archive after the proprietary period (normally one year after the data have been made available to the principal investigator) and all calibration data are public immediately after the observations.

¹<http://muse-vlt.eu/science/>

²The red giant branch phase is the stage of stellar evolution that follows the main sequence for low to intermediate-mass stars. During this phase the stellar atmosphere expands and the helium core contracts. This phase precedes the Helium burning phase.

³<http://archive.eso.org/cms/eso-data-access-policy.html>

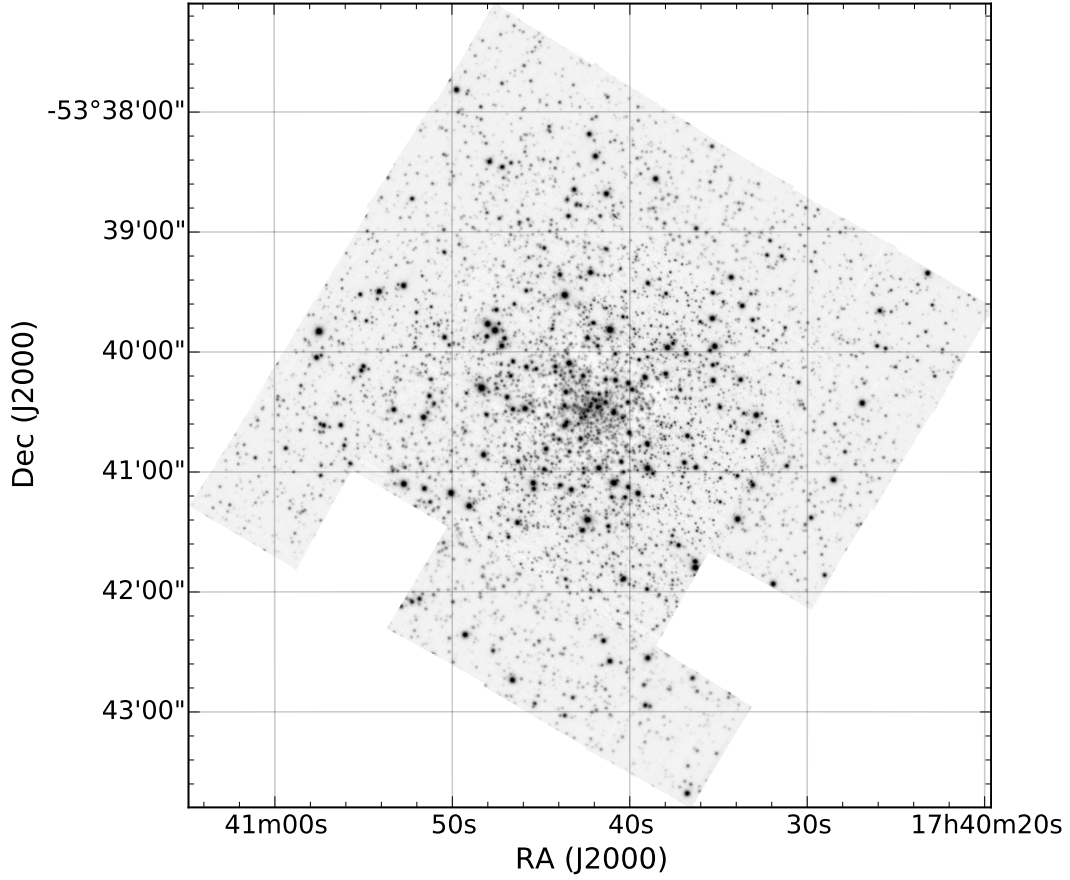


Figure 2.1: White image mosaic of MUSE data cubes of NGC 6397.

2.2.1 Data Reduction

I reduced the data with version 1.2.1 of the MUSE Instrument Pipeline Recipes⁴(Weilbacher et al., 2012). The pipeline distribution kit includes several packages. The ones used for this work are the following:

- The Common Pipeline Library version 6.6 (McKay et al., 2004)
- The ESO Recipe Execution Tool (EsoRex)⁵ version 3.12.

All the data reduction was done calling EsoRex to execute the MUSE DRS recipes from a bash (version 4.3.11) script⁶ (alternative this can be done via the Python bindings (Streicher & Weilbacher, 2012)). We summarize the main steps to produce the fully reduced data cube from the raw science and calibration data download from the ESO Science Archive MUSE Query Form. The data reduction

⁴The MUSE pipeline can be found at <http://www.eso.org/sci/software/pipelines/muse/>

⁵EsoRex is written by the CPL group (Pipeline System Department) European Southern Observatory <http://www.eso.org/sci/software/cpl/esorex.html>

⁶All the configuration files for each of the called MUSE recipes used, the bash scripts I wrote, useful python (Python 2.7.6) scripts, the scripts and data for all the plots produced and other text files generated during this internship relevant for the data reduction can be found at <https://github.com/manuelmarcano22/muse2016>

steps can be divided into two categories, pre-processing and post-processing. The pre-processing part includes all the necessary calibration to remove the instrument signature on the exposures. In the post-processing then the resulting pixel table for each science observation is calibrated for flux and astrometry, and then resample into a data cube.

1. Pre-processing

- I **Bias subtraction:** Bias subtraction was done by combining 10 different bias images into one master bias file. Each bias is part of the calibration files taken by ESO every night. A bias frame is dark image with no exposure time taken to account for the read out noise. (Recipe called *muse_bias*). For this and all subsequent steps we used a table of additional bad pixels of the CCDs created for the MUSE commission runs. This bad pixel table is distributed along with the MUSE pipeline files.
- II **Flat-fielding:** For the flat-field correction also 10 individual flat frames were combined into a master flat frame. The flat-field images are taken daily at the VLT as part of the standard calibration plan. The master flat contains the combined pixel values of the raw flat exposures. The purpose is to correct for uneven detector sensitivity. The recipe used was *muse_flat*. Besides the master flat, the recipe also produces a *trace table* containing polynomials defining the location of the slices on the CCD.
- III **Wavelength calibration:** For the wavelength calibration 15 different arc lamp exposures were used. These are 3 per lamp (Ne, Xe, HgCd lamps). The recipe used is *muse_wavcal*. It detects arc emission lines and determine the wavelength solution for each slice. The goal is to establish the pixel to wavelength equivalence with high precision.
- IV **Line Spread Function:** The line-spread function is calculated with the recipe *muse_lsf*. The lines spread function describes the broadening of spectral lines on a CCD. The recipe calculates this wavelength dependent function from 15 arc lamp exposures, and the wavelength solution calculated in the step above.
- V **Geometrical calibration:** In this step the recipe *muse_geometry* computes relative location of the slices within the field of view and measure the instrumental point spread function on the detectors. This creates a geometry table. A geometry table comes with the standard MUSE pipeline package as a static calibration files. The geometry table prepared for the third commissioning period was used in reducing the data.
- VI **Illumination Correction:** Flat-fields from the sky or twilight flats are taken weekly at the VLT. These are used to do large scale illumination correction. For the illumination correction also a special purpose illumination flat field called ILLUM can be used as an input to the recipe. These are taken throughout the observing night. We use the one taken closest in time to the science data. Both twilight flats and the ILLUM were used as input to the recipe *muse_twilight*.
- VII **Pixel table creation:** This step removes all the instrumental signatures on the science exposures and converts them from an image to a large table (called a pixel-table). Calling the recipe *muse_scibasic*, for each science frame a pixel table is created from the calibration file produced above (master bias, master flat, geometry table, bad pixel table, twilight correction). These tables are the input frames in the subsequent post-processing phase.

2. Post-processing

- I **Flux calibration:** In this step a flux response curve from a standard star exposure is created. The end product of the *muse_standard* are tables with the response curve as derived from standard star and the telluric absorption.
- II **Sky subtraction:** This step is only needed if the observed object fills the field of view. In the case of the NGC 6397 observation a reasonable sky spectrum can be obtained on the observation itself and use to subtract the sky.
- III **Astrometry:** An astrometry solution was done by the MUSE consortium for the third commissioning period. It ships with the muse pipeline and was the one used for the data astrometry correction.
- IV **Cube assembly:** In this last part a full data cube is created from a single exposure, the sky background is removed and the flux and the astrometric calibration are applied. In this step the cubes are sampled to a common value ($0''.2 \times 0''.2 \times 1.25 \text{Å}$). Individual data cubes from single exposures can be merged into a single data cube. This was done for each of the 23 different region of the cluster observed. For the center regions data cubes for the individual exposures were also created.

2.2.2 Spectral extraction and analysis

The spectral subtraction and analysis was carried out with a number of open-source scientific software. To visualize the data cubes and extract the spectra for analysis QFitsView⁷ was used. This is the graphical front-end written QT library of the DPUSER language. Spectral analysis and fitting was done with IRAF (Tody, 1986) (mainly through the command language based on Python PyRAF⁸) and Astropy (Astropy Collaboration et al., 2013). To calculate magnitudes the package Astrolib PySynphot (pysynphot) from the Space Telescope Science Institute was used and for plotting we made use of the APLpy package, an open-source plotting package for Python hosted at <http://aplpy.github.com>

⁷<http://www.mpe.mpg.de/~ott/QFitsView/>

⁸PyRAF is a product of the Space Telescope Science Institute operated for NASA by AURA

Chapter 3: Results

3.1 Cataclysmic Variables

From the population of known CV candidates in NGC 6397 we were able to get the spectra of five of them (see Fig. 3.1). In addition to recovering 3 of the previously detected cataclysmic variables, we have obtained the spectra for the first time of two CV candidates (U10 and U22 see figures 3.2 and 3.3). Their spectra confirms that these star are CVs, as suggested by their X-ray data (Grindlay et al., 2001). All the extracted spectra show the most common spectral lines detected from CVs. The most noticeable feature present in all the spectra being the Balmer lines. These are a set of spectral line emissions of the hydrogen atom. In the MUSE spectral range the $H\alpha$ (6562Å) and $H\beta$ (4861 Å) lines are detectable. These lines are known to show a double-peaked profile, characteristic of an accretion disc. The red and blue peaks are formed by the emission from the receding and approaching parts of the edge of an accretion disk. With the exception of U10, all the obtained spectra lie within a distance of 11" from the cluster center. Their spectra is obtained from two observing night of the cluster center. The total exposure time is 340 seconds from a total of 8 different exposures (4×25 s and 4×60 s). U10 lies at a distance of 1.21' and was also observed during two different nights. The total exposure time on U10 is 265 seconds divided in 9 short exposures (5×25 s and 4×35 s).

3.1.1 Variability

From the extracted CV spectra we calculated the magnitudes in the R band (in the VEGA system), and compare it to the magnitude seen in 2010 by the Hubble space telescope as reported by Cohn et al. (2010). The results are summarized in table 3.1. The CVs show moderate amplitude variability between the two observing times. This suggest that the majority of the CVs were observed during quiescence and not during an outburst. For some CVs like U22 where the change magnitude is bigger the possibility of being observed during outburst is not ruled out. A dwarf nova eruption can result in moderate magnitude changes of ~ 2 . This have been observed for U17 and U19. They have been reported to undergo dwarf nova eruptions with amplitudes of 1.8 and 2.7 magnitudes (Shara et al., 2005).

Based on data from dwarf novae in the field we can estimate how likely is that we have detected a CV during an outburst. About half of all know fields CVs are dwarf novae ($\sim 40\%$) and most discovered undergo 2-5 mag outburst (Downes et al., 2001; Warner, 2003). With data from the AAVSO catalog with a sample of 21 field DNs studied for an interval of three years Szkody & Mattei (1984) concluded that the probability of a DN being in quiescence at a random epoch is $\sim 85\%$. Due to the close distance to NGC 6397 we can make the assumption that we would have detected any outburst during the MUSE observation of the cluster. Based on this assumption we should have detected $\sim 15\%$ of the DN in NGC 6397. Even if we limit out sample size of potential DN to the 15 candidates we expect to see at least 1 CV in outburst during the observation.

3.1.2 Mass ratio

As seen in Figure 3.1 a common feature in all of the extracted spectra is the presence of the Balmer lines. We pay special attention to the $H\alpha$ when it is double peaked (see Fig 3.4). As show in Casares (2016) we can use the ratio of the double-peak separation (DP) to the full width half maximum (FWHM) of

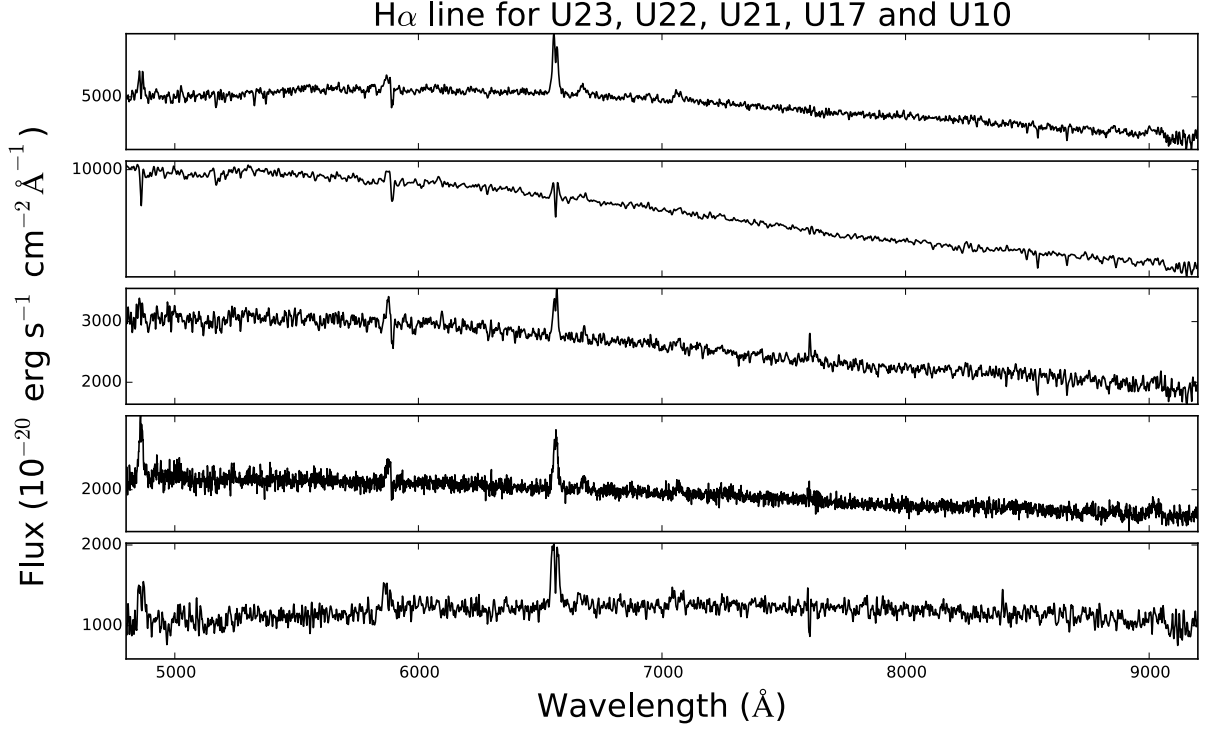


Figure 3.1: Obtained spectra from CVs in NGC 6397. Three of them have been previously identified as CVs: U23, U21 and U17 (Grindlay et al., 1995; Edmonds et al., 1999). U22 and U10 are CV candidates that have been first confirmed with spectroscopy. All CVs show strong Balmer lines (H α 6563 and H β 4861Å). The IDs are from (Bogdanov et al., 2010).

the H α emission line to get the mass ratio of the companion star to the compact object, q . This was done for CVs U23, U21 and U10 and the results are shown in fig 3.5.

3.1.3 Radial Velocity

With the 8 different exposures of the center region and the strong H α line emission the radial velocity evolution of the CV can be traced. This is done by employing the cross-correlation algorithms of Tonry & Davis (1979), as implemented in the IRAF Radial Velocity Analysis Package. This was done for U23, one of the brightest and one of the only two CVs in NGC 6397 for which the period have been measured (Kaluzny & Thompson, 2003). The resulting radial velocity evolution is plotted in Figure ?? . The first exposure of 25 second for the first night was used as the template to calculate radial velocity shift. No significant radial velocity was detected. The same procedure to determine the radial velocity shift between the combine exposures for the first night and for the second observing night.

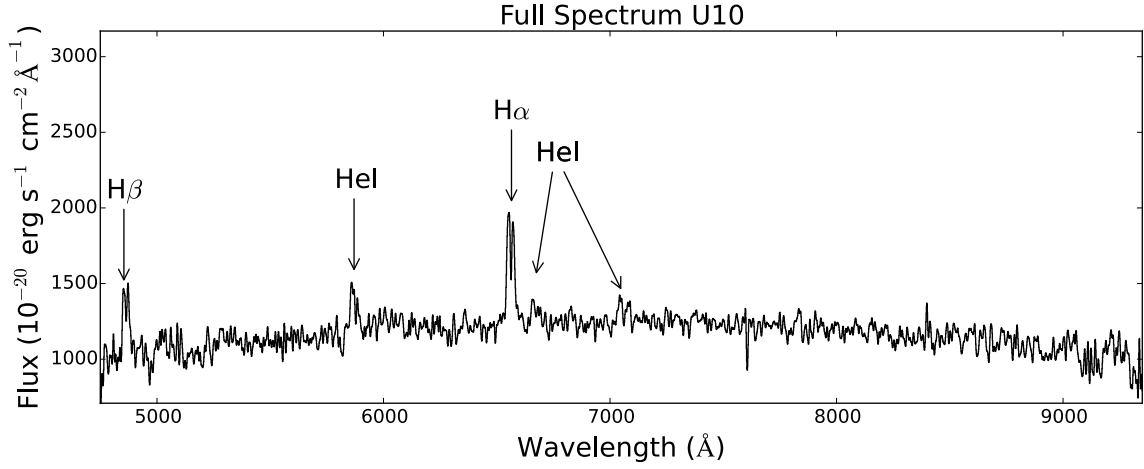


Figure 3.2: Spectrum of U23 with strong Hydrogen double peaked emission (characteristic of an accretion disk), and a strong Helium I lines.

CV	R Magnitude (2014)	R (Cohn et al. 2010)
U17	20.12	18.52
U23	19.15	17.88
U10	20.7	19.14
U21	19.79	19.82
U22	18.54	20.15

Table 3.1: Magnitudes in the R band for the 5 CVs detected by MUSE in 2014 and the R magnitudes in 2010 studied by Cohn et al. (2010). Some CVs show small magnitude variability between the two epochs (~ 1 magnitude).

3.2 Low-mass X-ray Binary

Besides the population of CVs in NGC 6397 we also studied a LMXB located near the center in NGC 6397. The goal was to detect possible $H\alpha$ emission from the LMXB. The detection of hydrogen lines in the LMXB will remove any ambiguities regarding the composition of the neutron star atmosphere. The absence of hydrogen will be an argument for using a Helium atmosphere model giving different mass-radius relation than for a hydrogen one. This will help better constraint the equation of state of neutron stars. Using all the available observations of the center, we estimated the flux in the $H\alpha$ band to be 8.2×10^{-18} erg/s/cm². This is a very faint object (R magnitude of ~ 26 (Heinke et al., 2014)). More integration time is needed to be able to get a spectra with a good signal-to-noise ratio and study the spectra of the LMXB.

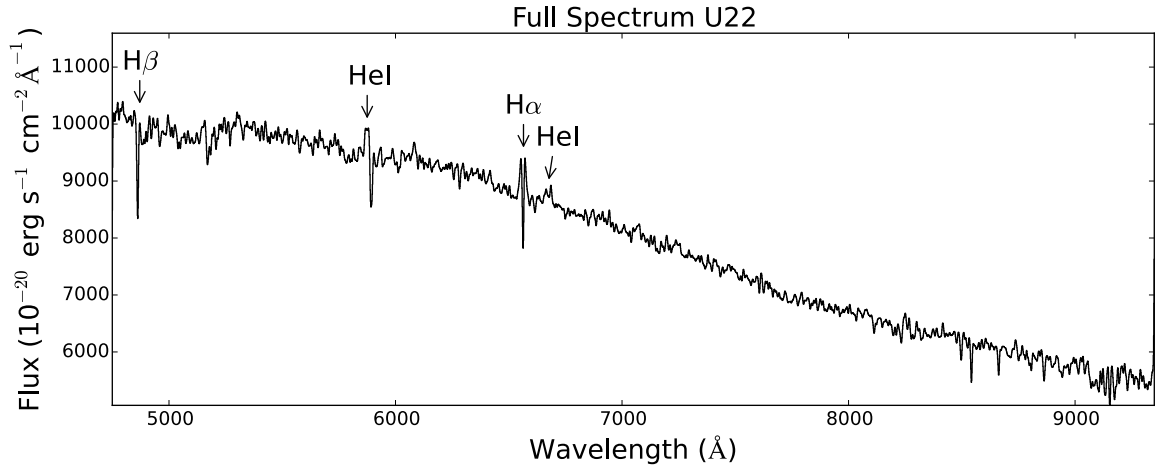


Figure 3.3: Spectrum of U22 with strong $\text{H}\alpha$ double peaked emission, absorption in the $\text{H}\beta$ line, and Helium I lines.

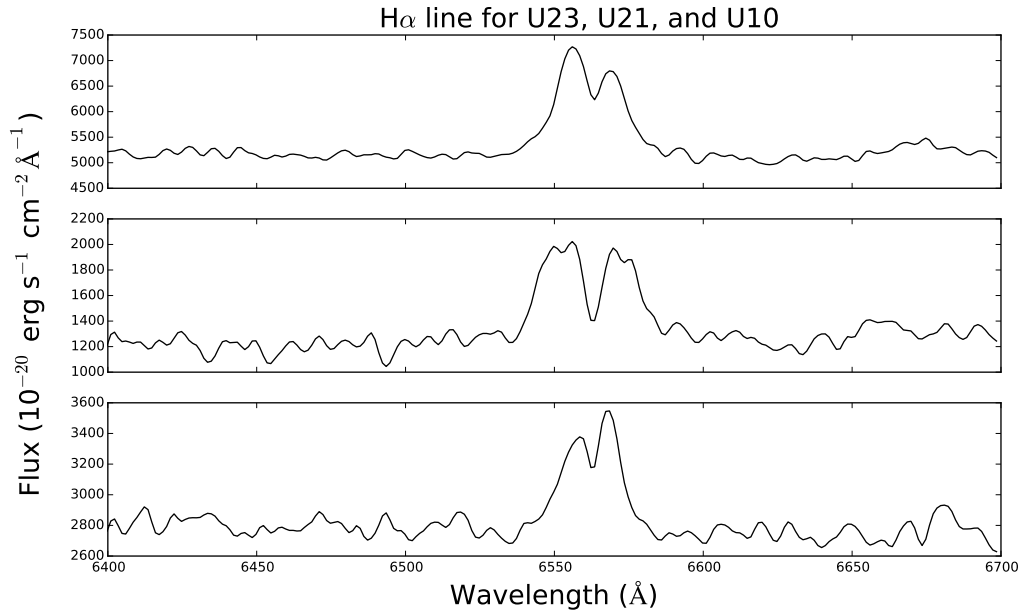


Figure 3.4: Zoom of the spectra around $\text{H}\alpha$ for U23 (top), U21 (middle), and U10 (bottom)

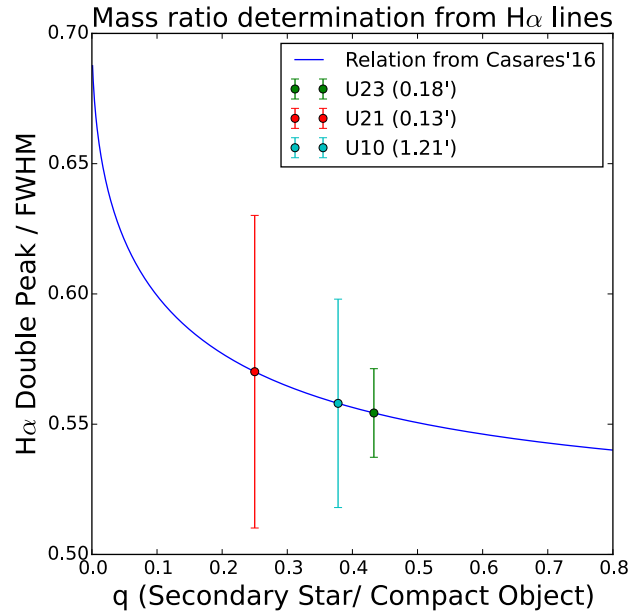


Figure 3.5: The solid line is the relation between the ratio of $H\alpha$ double peak separation to Full width at half maximum (FWHM) and the mass ratio q (companion star over white dwarf mass) from Casares (2016). Our measured values for the CVs are shown as points with their error bars. The value in parenthesis is the projected distance to the cluster center for each CV. q for U23 is 0.433, for U21 is 0.25 and 0.3 for U10.

Chapter 4: Discussion and Conclusions

To finish we come back to the four open questions about CVs in globular clusters discussed in the introduction.

4.1 Primordial CVs

In this work we studied the population of CVs in NGC 6397. Previous photometric and X-ray studies of this cluster have identified a sample of 15 CV candidates. In this work we located the candidates on the MUSE observations to examine their spectral signature and extent the sample of spectroscopically confirmed CV candidates. From the sample we were able to unambiguously identify 5 CVs via their bright $H\alpha$ line in emission, sign of an accretion disk. We have obtained the spectra of two new CVs, one of the spectra being the first one from a CV outside the cluster center. Increasing the sample size of CV spectra, and looking at the CVs in different locations in the cluster, increases the chances of detecting the predicted populations of CVs. For the CV candidates farther from the cluster center (with one exception) no $H\alpha$ line was detected. This suggest that these might belong to a different kind of 'faint' CV population. Their radial distribution and their weak $H\alpha$ emission might suggest that these are primordial CVs. CVs from primordial origins are expected to be near the minimum period and have their optical spectra dominated by the white dwarf as the companion is a highly evolved and drained main sequence star. An hydrogen emission is still expected but probably weakened and inside broad absorption lines signature of a white dwarf. The lack of bright hydrogen lines from these object also leaves the door open to the possibility of seen white dwarfs accreting from helium dwarf companion. This are of great as gravitational waves sources for futures missions like eLISA. Such types of CVs have never been identify in globular clusters although they are predicted to exist. Deeper observation will MUSE are needed to get spectra with good signal-to-noise ratio and correctly classify them as such.

Studying the companion stars of the CVs can also give us a clue about primordial CVs, as dynamically formed CVs are expected to have a bias towards having a more massive companion. On none of the obtained spectra we observed signature of a M star (TiO lines e.g (Marsh, 1990)). This suggest that the companion stars might possibly be a K type star ($0.54 - 0.9M_{\odot}$ (Gray, 2005)). Knowing that the turnoff mass ¹ is $0.77M_{\odot}$ for NGC 6397 (De Marco et al., 2005). This gives us a range of $\sim 0.5 - 0.8M_{\odot}$. Leaving the possibility for the companion to be either a M type star or even a low mass white dwarf or helium dwarf.

4.2 Periods

As mentioned before the $H\alpha$ emission line was used to detect radial velocity variations in the CVs. Since the period of U23 is known, we used it as a check if radial velocity could be detected in the short exposures taken by MUSE. However, since the method depends on the strength of the emission line (and the integration time required to detect it significantly), the short exposures available were not enough to be able to unambiguously detect radial velocity shifts. This suggest that longer integration time (> 25 seconds) is needed to be able to determine the period of the CVS in NGC 6397 with

¹the turn off mass is the maximum mass on the main sequence. This can serve as a rough estimate of the maximum mass of main sequence stars in a globular clusters.

the MUSE instrument. Exposures of a few minutes ($\sim 6m$) with the data of two separated nights combined a determination of radial velocity shift could be done. With longer exposures spread apart of globular clusters MUSE would be able to trace simultaneously the radial velocity shift of multiple objects allowing the possibility of the determination of the orbital parameters of binaries in globular clusters. This is of great interest as the number of CVs in globular clusters is very low.

4.3 Magnetism and dwarf novae

As mentioned before it has been proposed that the majority of CVs in globular clusters are magnetic (Grindlay, 1999). For NGC 6397, remarkably, all 4 previously identified CVs show prominent Helium II lines. These line are generally associated with magnetic and nova-like CVs (Echevarria, 1988). We did not detect any Helium II line in any of the two newly studied spectra (U10 and U22). This might suggest that they are not magnetic in nature. However, this is not conclusive as the strongest He II line is outside of the MUSE spectral range (4686\AA). This means that the possibility that the two newly identified CVs are magnetic have not been completely ruled out.

Regarding the dwarf novae, U22 showed a moderate increase in magnitude compared to previous observation. This is not irrefutable evidence that U22 was observed during an outburst and photometric follow up to study the variability is needed for confirmation. If U22 is indeed a dwarf novae it would be the third one identify in NGC 6397 (Shara et al., 2005) and contribute to the still small sample of DN outburst spectra (37 out of 1600 CVs (Downes et al., 2001)). The fact that only one DN in outburst candidate was identify supports the claim made by Shara et al. (1996) that DNs are very rare in globular clusters. There are many caveats with the assumptions made as the estimated rates of DN are mainly empirical and can suffer from selection bias due to the fact that observations of bright and long period outbursts are easier to detect.

Altogether we have demonstrated how an IFU like MUSE can be used to study the population of compact objects in globular clusters. Here we exposed some hints that field CVs and GC population are different and the dynamics of the overall globular cluster plays a role on the formation of compact objects. Deeper observations at different epochs is needed to constraint the current models on the evolution of globular clusters and formation of binaries in them. MUSE is a well fitted instrument for the task as it allows to study the variability and spectral features of a high number of objects simultaneously. This open the way for the discovery of new objects in globular clusters and increase our understating on them and their constituents. For this work we were limited by the very short exposure times. This is mainly because these observations took place during the commissioning period and so were constrained by the overall commission goals. MUSE is now in regular observation time and among its future and current targets there is a number of other galactic globular cluster. Also improvement in the instrument are expected soon, like for example the use of adaptive optic and the narrow field mode. This means a vast number of new data set that can be exploited to improve our understanding on the formation of compact objects in globular clusters.

Chapter 5: Future Work

5.1 Follow up Observation

Observing time to study the neutron star low-mass X-ray binary in NGC 6397 with MUSE have been requested with Dr. Sebastien Guillot as the principal investigator. The goal is to constraint the equation of state of neutron stars by syduin the $H\alpha$ line emission from the LMXB to be able to correctly model the atmosphere model.

Since MUSE have a big field of view and the LMXB is close to the cluster center, the observation will allow us to study also the CV population at the center. As a secondary objective, the long exposure of the core of NGC 6397 will allow a much deeper study of the sources in the cluster core. Moreover if $H\alpha$ line is detected the observation could be split to detect radial velocity variations. The big field of view will allow for the determination of the radial velocity shift in both the LMXB and the CVs.

5.2 Data analysis

5.2.1 Optimal Spectra Extraction

The spectral extraction was done with QFitsView by adding the spectra from four adjacent pixels from identified source in the datacube. QFitView allows to vary the number of pixels to add, and to obtain the spectra from the mean or median of the selected number of adjacent pixels. . The number of pixels to add were determined by visual examination of the spectra. A more systematic way was shown by Horne & Marsh (1986). This can potentially increase the quality of the extracted spectra.

5.2.2 Short Term variability

Besides the radial velocity shift with the individual short exposures we can examine the short term variability of the CVs. This can be done for the bright enough sources detectable in the short 25 seconds exposures. We plan to study the variations in the flux of strong emission lines like the $H\alpha$ line. This can help us determine the magnetic nature of the CVs as magnetic CVs are expected to be more variable in short timescales.

5.2.3 Processed data

As it was mentioned before the data for over 14000 extracted spectra from the MUSE observation of NGC 6397 is available online. This only include the extracted spectra with $SNR > 5$ and mainly includes main sequence stars, but a thoroughly search of can be done to identify possible binaries in the data set. The plan would be to examine the dataset looking for strong $H\alpha$ emitters as signs of an accretion disk. The data was extracted with a program developed by Sebastien Kamann called PAMPLEMUSE (Kamann et al., 2013). This method can be use to search in NGC 6397 and in futures observations of globular clusters with MUSE to identify prospects compact binaries candidates.

5.3 Reproducibility

5.3.1 Continuous Analysis

Being able to replicate and validate previous results is in the heart of science. When computer and data are involved this means to ensure access to the raw data and the workflow. One way of ensuring reproducibility on research areas involving computer work is creating an isolated computational environment that captures the versions and dependencies of all the used libraries and programs. Dockers¹ containers are an open source alternative that provides a fast and lightweight way to isolate the computational environment in which the data reduction and analysis was done. This avoids any future dependencies or version conflicts and allows the work to be portable and easily reproduced for validation or improvements in any operating system. Recently the term 'continuous analysis' was introduced for container-based research flows if they include version control and specially continuous integration, a well established software development technique. The details are outlined in Beaulieu-Jones & Greene (2016). The plan is to adopt such workflows for future work done.

5.3.2 Cloud Computing

Another challenge for astronomical data that applies for MUSE data is how computationally demanding their processing is. For example, the recommended memory for a machine for creating the final data cube from a single MUSE observation and the required set of calibrations is 64 GB of memory. The same applies for the number of CPU cores and disk space. This is why the data reduction work was done in an institutional server with the minimum requirements. This is not optimal for portability and reproducibility. One option is to make use of a cloud computing environment, such as provided by the Amazon Web Service (AWS) that provide on-demand access to large-scale computational resources. An example of something like this done in academia for reproducibility goals is the work of Ragan-Kelley et al. (2013). More recently in astrophysics this approach has been explored by members of the Square Kilometer Array organization and members of the project CHILES. See Dodson et al. (2016) for the details.

¹<https://www.docker.com/>

Bibliography

- Antonov, V. A. 1962, Solution of the problem of stability of stellar system Emden's density law and the spherical distribution of velocities
- Astropy Collaboration, Robitaille, T. P., Tollerud, E. J., Greenfield, P., Droettboom, M., Bray, E., Aldcroft, T., Davis, M., Ginsburg, A., Price-Whelan, A. M., Kerzendorf, W. E., Conley, A., Crighton, N., Barbary, K., Muna, D., Ferguson, H., Grollier, F., Parikh, M. M., Nair, P. H., Unther, H. M., Deil, C., Woillez, J., Conseil, S., Kramer, R., Turner, J. E. H., Singer, L., Fox, R., Weaver, B. A., Zabalza, V., Edwards, Z. I., Azalee Bostroem, K., Burke, D. J., Casey, A. R., Crawford, S. M., Dencheva, N., Ely, J., Jenness, T., Labrie, K., Lim, P. L., Pierfederici, F., Pontzen, A., Ptak, A., Refsdal, B., Servillat, M., & Streicher, O. 2013, *Astronomy and Astrophysics*, 558, A33
- Bacon, R., Accardo, M., Adjali, L., Anwand, H., Bauer, S., Biswas, I., Blaizot, J., Boudon, D., Brau-Nogue, S., Brinchmann, J., Caillier, P., Capoani, L., Carollo, C. M., Contini, T., Couderc, P., Daguisé, E., Deiries, S., Delabre, B., Dreizler, S., Dubois, J., Dupieux, M., Dupuy, C., Emsellem, E., Fechner, T., Fleischmann, A., François, M., Gallou, G., Gharsa, T., Glindemann, A., Gojak, D., Guiderdoni, B., Hansali, G., Hahn, T., Jarno, A., Kelz, A., Koehler, C., Kosmalski, J., Laurent, F., Le Floch, M., Lilly, S. J., Lizon, J.-L., Loupiau, M., Manescau, A., Monstein, C., Nicklas, H., Olaya, J.-C., Pares, L., Pasquini, L., Pécontal-Rousset, A., Pelló, R., Petit, C., Popow, E., Reiss, R., Remillieux, A., Renault, E., Roth, M., Rupprecht, G., Serre, D., Schaye, J., Soucail, G., Steinmetz, M., Streicher, O., Stuik, R., Valentin, H., Vernet, J., Weilbacher, P., Wisotzki, L., & Yerle, N. 2010, in *Proceedings of the SPIE*, Vol. 7735, *Ground-based and Airborne Instrumentation for Astronomy III*, 773508
- Bacon, R., Vernet, J., Borisova, E., Bouche, N., Brinchmann, J., Carollo, M., Carton, D., Caruana, J., Cerda, S., Contini, T., Franx, M., Girard, M., Guérou, A., Haddad, N., Hau, G., Herenz, C., Herrera, J. C., Husemann, B., Husser, T.-O., Jarno, A., Kamann, S., Krajnovic, D., Lilly, S., Mainieri, V., Martinsson, T., Palsa, R., Patricio, V., Pecontal, A., Pello, R., Piqueras, L., Richard, J., Sandin, C., Schroetter, I., Selman, F., Shirazi, M., Smette, A., Soto, K., Streicher, O., Urrutia, T., Weilbacher, P., Wisotzki, L., & Zins, G. 2014, *The Messenger*, 157, 13
- Balman, S. 2012, *Memorie della Societa Astronomica Italiana*, 83, 585
- Barden, S. C., Arns, J. A., & Colburn, W. S. 1998, in *Proceedings of the SPIE*, Vol. 3355, *Optical Astronomical Instrumentation*, ed. S. D'Odorico, 866–876
- Beaulieu-Jones, B. K. & Greene, C. S. 2016, *bioRxiv*
- Bogdanov, S., Berg, M. v. d., Heinke, C. O., Cohn, H. N., Lugger, P. M., & Grindlay, J. E. 2010, *The Astrophysical Journal*, 709, 241
- Brown, G., Lee, C.-H., Wijers, R., & Bethe, H. 2000, *Physics Reports*, 333-334, 471
- Cannizzo, J. K. & Mattei, J. A. 1998, *The Astrophysical Journal*, 505, 344
- Casares, J. 2016, *The Astrophysical Journal*, 822, 99

- Chandrasekhar, S. 1931, *The Astrophysical Journal*, 74, 81
- Cohn, H. N., Lugger, P. M., Couch, S. M., Anderson, J., Cool, A. M., van den Berg, M., Bogdanov, S., Heinke, C. O., & Grindlay, J. E. 2010, *The Astrophysical Journal*, 722, 20
- Cool, A. M., Grindlay, J. E., Cohn, H. N., Lugger, P. M., & Slavin, S. D. 1995, *The Astrophysical Journal*, 439, 695
- Cool, A. M., Grindlay, J. E., Krockenberger, M., & Bailyn, C. D. 1993, *The Astrophysical Journal Letters*, 410, L103
- Coppejans, D. L., Koerding, E. G., Miller-Jones, J. C. A., Rupen, M. P., Knigge, C., Sivakoff, G. R., & Groot, P. J. 2015, arXiv:1506.00003 [astro-ph], arXiv: 1506.00003
- Cropper, M. 1990, *Space Science Reviews*, 54
- de Boer, K. & Seggewiss, W. 2008, *Stars and Stellar Evolution* (EDP Sciences)
- De Loore, C. W. H. & Doom, C. 1992, *Astrophysics and Space Science Library*, Vol. 179, *Structure and Evolution of Single and Binary Stars* (Dordrecht: Springer Netherlands)
- De Marco, O., Shara, M. M., Zurek, D., Ouellette, J. A., Lanz, T., Saffer, R. A., & Sepinsky, J. F. 2005, *The Astrophysical Journal*, 632, 894
- Dodson, R., Vinsen, K., Wu, C., Popping, A., Meyer, M., Wicenec, A., Quinn, P., van Gorkom, J., & Momjian, E. 2016, *Astronomy and Computing*, 14, 8
- Downes, R. A., Webbink, R. F., Shara, M. M., Ritter, H., Kolb, U., & Duerbeck, H. W. 2001, *The Publications of the Astronomical Society of the Pacific*, 113, 764
- Duncan, R. C. & Thompson, C. 1992, *The Astrophysical Journal*, 392, L9
- Echevarria, J. 1988, *Monthly Notices of the Royal Astronomical Society*, 233, 513
- Edmonds, P. D., Grindlay, J. E., Cool, A., Cohn, H., Lugger, P., & Bailyn, C. 1999, *The Astrophysical Journal*, 516, 250
- Fowler, R. H. 1926, *Monthly Notices of the Royal Astronomical Society*, 87, 114
- Frank, J., King, A., & Raine, D. J. 2002, *Accretion Power in Astrophysics: Third Edition* (Cambridge University Press)
- Gehrz, R. D., Truran, J. W., Williams, R. E., & Starrfield, S. 1998, *Publications of the Astronomical Society of the Pacific*, 110, 3
- Gray, D. 2005, *The Observation and Analysis of Stellar Photospheres* (Cambridge University Press)
- Grindlay, J. E. 1999, in , eprint: arXiv:astro-ph/9901356, 377
- Grindlay, J. E. 2006, *Advances in Space Research*, 38, 2923
- Grindlay, J. E., Cool, A. M., Callanan, P. J., Bailyn, C. D., Cohn, H. N., & Lugger, P. M. 1995, *The Astrophysical Journal Letters*, 455, L47

- Grindlay, J. E., Heinke, C. O., Edmonds, P. D., Murray, S. S., & Cool, A. M. 2001, *The Astrophysical Journal Letters*, 563, L53
- Hamada, T. & Salpeter, E. E. 1961, *The Astrophysical Journal*, 134, 683
- Harris, W. E. 1996, *The Astronomical Journal*, 112, 1487
- Heger, A., Fryer, C. L., Woosley, S. E., Langer, N., & Hartmann, D. H. 2003, *The Astrophysical Journal*, 591, 288
- Heinke, C. O., Cohn, H. N., Lugger, P. M., Webb, N. A., Ho, W. C. G., Anderson, J., Campana, S., Bogdanov, S., Haggard, D., Cool, A. M., & Grindlay, J. E. 2014, *Monthly Notices of the Royal Astronomical Society*, 444, 443
- Hewish, A., Bell, S. J., Pilkington, J. D. H., Scott, P. F., & Collins, R. A. 1968, *Nature*, 217, 709
- Horne, K. & Marsh, T. R. 1986, *Monthly Notices of the Royal Astronomical Society*, 218, 761
- Husser, T.-O., Kamann, S., Dreizler, S., Wendt, M., Wulff, N., Bacon, R., Wisotzki, L., Brinchmann, J., Weilbacher, P. M., Roth, M. M., & Monreal-Ibero, A. 2016, *Astronomy and Astrophysics*, 588, A148
- Hut, P., McMillan, S., Goodman, J., Mateo, M., Phinney, E. S., Pryor, C., Richer, H. B., Verbunt, F., & Weinberg, M. 1992, *Publications of the Astronomical Society of the Pacific*, 104, 981
- Ivanova, N., Belczynski, K., Fregeau, J. M., & Rasio, F. A. 2005, *Monthly Notices of the Royal Astronomical Society*, 358, 572
- Ivanova, N., Heinke, C. O., Rasio, F. A., Taam, R. E., Belczynski, K., & Fregeau, J. 2006, *Monthly Notices of the Royal Astronomical Society*, 372, 1043
- Kaluzny, J. & Thompson, I. B. 2003, *The Astronomical Journal*, 125, 2534
- Kaluzny, J., Thompson, I. B., Krzeminski, W., & Schwarzenberg-Czerny, A. 2006, *Monthly Notices of the Royal Astronomical Society*, 365, 548
- Kamann, S., Husser, T.-O., Brinchmann, J., Emsellem, E., Weilbacher, P. M., Wisotzki, L., Wendt, M., Krajnović, D., Roth, M. M., Bacon, R., & Dreizler, S. 2016, *ArXiv e-prints*, 1602, arXiv:1602.01643
- Kamann, S., Wisotzki, L., & Roth, M. M. 2013, *Astronomy & Astrophysics*, 549, A71
- Kepler, S. O. & Bradley, P. A. 1995, *Baltic Astronomy*, 4
- King, I. R. 1966, *The Astronomical Journal*, 71, 64
- Kinney, A. 1994, in *Astronomical Society of the Pacific Conference Series*, Vol. 54, *The Physics of Active Galaxies*, ed. G. V. Bicknell, M. A. Dopita, & P. J. Quinn, 61
- Kippenhahn, R., Kohl, K., & Weigert, A. 1967, *Zeitschrift für Astrophysik*, 66
- Knigge, C. 2012, *Memorie della Societa Astronomica Italiana*, 83
- Koester, D. & Chanmugam, G. 1990, *Reports on Progress in Physics*, 53, 837

- Koester, D. & Weidemann, V. 1980, *Astronomy and Astrophysics*, 81
- Kopal, Z. 1955, *Annales d'Astrophysique*, 18
- . 1959, *Close binary systems* (New York: Wiley)
- Körding, E., Rupen, M., Knigge, C., Fender, R., Dhawan, V., Templeton, M., & Muxlow, T. 2008, *Science*, 320, 1318
- Krzeminski, W. & Serkowski, K. 1977, *The Astrophysical Journal*, 216, L45
- Lattimer, J. M. & Prakash, M. 2007, *Physics Reports*, 442, 109
- Lubow, S. H. & Shu, F. H. 1975, *The Astrophysical Journal*, 198, 383
- Lynden-Bell, D. & Eggleton, P. P. 1980, *Monthly Notices of the Royal Astronomical Society*, 191, 483
- Lynden-Bell, D. & Pringle, J. E. 1974, *Monthly Notices of the Royal Astronomical Society*, 168, 603
- Lynden-Bell, D. & Wood, R. 1968, *Monthly Notices of the Royal Astronomical Society*, 138, 495
- Maccarone, T. & Knigge, C. 2007, *Astronomy and Geophysics*, 48, 5.12
- Madsen, J. 1999, in *Hadrons in Dense Matter and Hadrosynthesis*, ed. J. Cleymans, H. B. Geyer, & F. G. Scholtz, Vol. 516 (Berlin, Heidelberg: Springer Berlin Heidelberg), 162–203
- Marsh, T. R. 1990, *Astrophysical Journal*, 357, 621
- McKay, D. J., Ballester, P., Banse, K., Izzo, C., Jung, Y., Kiesgen, M., Kornweibel, N., Lundin, L. K., Modigliani, A., Palsa, R. M., & Sabet, C. 2004, in , 444–452
- McLaughlin, D. E. & van der Marel, R. P. 2005, *The Astrophysical Journal Supplement Series*, 161, 304
- Meylan, G. & Heggie, D. C. 1997, *Astronomy and Astrophysics Reviews*, 8, 1
- Oppenheimer, J. R. & Volkoff, G. M. 1939, *Physical Review*, 55, 374
- Osaki, Y. 1974, *Publications of the Astronomical Society of Japan*, 26, 429
- Patterson, J. 1994, *Publications of the Astronomical Society of the Pacific*, 106, 209
- Postnov, K. A. & Yungelson, L. R. 2014, *Living Reviews in Relativity*, 17
- Prada Moroni, P. G. & Straniero, O. 2009, *Astronomy and Astrophysics*, 507, 1575
- Ragan-Kelley, B., Walters, W. A., McDonald, D., Riley, J., Granger, B. E., Gonzalez, A., Knight, R., Perez, F., & Caporaso, J. G. 2013, *The ISME Journal*, 7, 461
- Reisenegger, A. 2005, in (AIP), 263–273
- Rhoades, C. E. & Ruffini, R. 1974, *Physical Review Letters*, 32, 324
- Robinson, E. L. 1983, in *Astrophysics and Space Science Library*, Vol. 101, IAU Colloq. 72: Cataclysmic Variables and Related Objects, ed. M. Livio & G. Shaviv, 1–14

- Schuerman, D. W. 1972, *Astrophysics and Space Science*, 19, 351
- Shara, M. M. 1989, *Publications of the Astronomical Society of the Pacific*, 101, 5
- Shara, M. M., Bergeron, L. E., Gilliland, R. L., Saha, A., & Petro, L. 1996, *Astrophysical Journal*, 471, 804
- Shara, M. M., Hinkley, S., Zurek, D. R., Knigge, C., & Dieball, A. 2005, *The Astronomical Journal*, 130, 1829
- Starrfield, S., Iliadis, C., & Hix, W. R. 2016, *Publications of the Astronomical Society of the Pacific*, 128, 051001
- Streicher, O. & Weilbacher, P. M. 2012, *Astronomical Data Analysis Software and Systems XXI*, 461
- Suh, I.-S. & Mathews, G. J. 2000, *The Astrophysical Journal*, 530, 949
- Szkody, P. & Mattei, J. A. 1984, *Publications of the Astronomical Society of the Pacific*, 96, 988
- Tapia, S. 1977, *The Astrophysical Journal*, 212, L125
- Tauris, T. M. & van den Heuvel, E. P. J. 2006, in *Compact stellar X-ray sources*, 623–665
- Taylor, J. M., Grindlay, J. E., Edmonds, P. D., & Cool, A. M. 2001, *The Astrophysical Journal Letters*, 553, L169
- Tody, D. 1986, in *Proceedings of the SPIE*, Vol. 627, *Instrumentation in astronomy VI*, ed. D. L. Crawford, 733
- Tonry, J. & Davis, M. 1979, *Astronomical Journal*, 84, 1511
- van den Heuvel, E. P. J. 1976, in *IAU Symposium*, Vol. 73, *Structure and Evolution of Close Binary Systems*, ed. P. Eggleton, S. Mitton, & J. Whelan, 35
- Verbunt, F. 1982, *Space Science Reviews*, 32
- Verbunt, F., Bunk, W. H., Ritter, H., & Pfeffermann, E. 1997, *Astronomy and Astrophysics*, 327
- Warner, B. 2003, *Cataclysmic Variable Stars* (Cambridge University Press)
- Weilbacher, P. M., Streicher, O., Urrutia, T., Jarno, A., Pécontal-Rousset, A., Bacon, R., & Böhm, P. 2012, 84510B
- Wickramasinghe, D. T. & Ferrario, L. 2000, *Publications of the Astronomical Society of the Pacific*, 112, 873
- Zavlin, V. E., Pavlov, G. G., & Shibano, Y. A. 1996, *Astronomy and Astrophysics*, 315, 141